

Elliptic flow of colored glass in high energy heavy ion collisions

Alex Krasnitz,¹ Yasushi Nara,² and Raju Venugopalan^{3,2}

¹*FCT and CENTRA, Universidade do Algarve, Campus de Gambelas, P-8000 Faro, Portugal*

²*RIKEN BNL Research Center, Brookhaven National Laboratory, Upton, N.Y. 11973, U.S.A.*

³*c Physics Department, Brookhaven National Laboratory, Upton, N.Y. 11973, U.S.A.*

(Dated: January 25, 2019)

We compute the elliptic flow generated by classical gluon fields in a high energy nuclear collision. A significant elliptic flow is generated over time scales on the order of the system size. The flow is dominated by soft modes which linearize only at very late times.

The collective flow of excited nuclear matter has been an important tool in attempts to extract the nuclear equation of state ever since the early days of heavy ion collision experiments [1]. Measurements of collective flow at the Relativistic Heavy Ion Collider (RHIC) may provide insight into the excited partonic matter, often called a Quark Gluon Plasma (QGP), produced in high energy heavy ion collisions [2]. In particular, the azimuthal anisotropy in the transverse momentum distribution has been proposed as a sensitive probe of the hot and dense matter produced in ultra-relativistic heavy ion collisions [3]. A measure of the azimuthal anisotropy is the second Fourier coefficient of the azimuthal distribution, the elliptic flow parameter v_2 . Its definition is [4]

$$v_2 = \langle \cos(2\phi) \rangle = \frac{\int_{-\pi}^{\pi} d\phi \cos(2\phi) \int d^2p_T \frac{d^3N}{dy d^2p_T d\phi}}{\int_{-\pi}^{\pi} d\phi \int d^2p_T \frac{d^3N}{dy d^2p_T d\phi}}. \quad (1)$$

The elliptic flow for non-central collisions is believed to be sensitive to the early evolution of the system [5].

The first measurements of elliptic flow from RHIC, at center of mass energy $\sqrt{s_{NN}} = 130$ GeV, have been reported recently [6]. Hydrodynamic model calculations provide good agreement, for large centralities, and for particular initial conditions and equations of state, with the measured centrality dependence of the data [8]. The agreement at smaller centralities is less good, perhaps reflecting the breakdown of a hydrodynamic description in smaller systems [9]. Hydrodynamic models also agree well with the p_T dependence of the unintegrated (see Eq. (1)) elliptic flow parameter $v_2(p_T)$ up to 1.5 GeV/c at mid-rapidity [8]. However, above 1.5 GeV, the experimental distribution appears to saturate, while the hydrodynamic model distributions continue to rise [8]. Jet quenching scenarios to explain this saturated behavior of $v_2(p_T)$ at large p_T [10] appear to disagree quantitatively with the data. Partonic transport models including only elastic gluon-gluon scattering require large cross sections or large initial gluon number to obtain significant elliptic flow [11].

In this letter, we compute the contribution to v_2 at central rapidities from the strong color fields generated in the initial instants after the heavy ion collision. These are generated as follows. At high energies, or equivalently, at small Broken x , the parton density in a nucleus

grows very rapidly and saturates eventually [12] forming a Color Glass Condensate [13] (CGC). The CGC is characterized by the color charge squared per unit area Λ_s^2 which grows with energy, centrality and the size of the nuclei. Estimates for RHIC give $\Lambda_s \sim 1.4 - 2$ GeV [15]. For a recent review of the CGC model and additional references, see Ref. [14]. Since the occupation number of gluons in the CGC is large, $f \sim 1/\alpha_S(\Lambda_s^2) > 1$, classical methods can be applied to study gluon production in heavy ion collisions at high energies [18, 19]. The energy and number [20, 21] of gluons produced were computed numerically for an SU(2) Yang-Mills gauge theory and recently extended to the SU(3) case [22]. We have confirmed that strong electric and magnetic fields of order $1/\alpha_S$ are generated in a time $\tau \sim 1/\Lambda_s$ after the collision.

The classical Yang-Mills approach may be applied to compute elliptic flow in a nuclear collision [23]. As in our earlier work, we assume strict boost invariance. The dynamics is then that of a Yang-Mills gauge field coupled to an adjoint scalar field in 2+1-dimensions. For a numerical solution we use lattice discretization. The discretized theory is described by a Kogut-Susskind Hamiltonian [20].

In previous work, we studied gluon production in central collisions of very large nuclei and therefore assumed a uniform color charge distribution in the transverse plane. To study effects of anisotropy and spatial inhomogeneity, we shall consider a finite nucleus. We shall impose suitable neutrality conditions on the distribution of color sources [24] to prevent gluon production at large distances outside the nucleus.

To this end, we model a nucleus as a sphere of radius R , filled with randomly distributed nucleons of radius $l \approx 1$ fm. For a gold nucleus, $R \approx 6.5$ fm. The color charge distribution within a nucleon is generated as follows. First, we generate (throughout the transverse plane of a nucleon) a random uncorrelated Gaussian distribution $\rho^a(\vec{r})$ (a being the adjoint color index and \vec{r} the transverse-plane position vector), obeying the relation $\langle \rho^a(\vec{r}) \rho^b(\vec{r}') \rangle = \Lambda_n^2 \delta^{ab} \delta(\vec{r} - \vec{r}')$ where the $\langle \rangle$ average is over the ensemble of nucleons. Next, we remove the monopole and dipole components of the distribution by superimposing the distribution with the appropriate homogeneous contribution; first of the color charge, then

of the color dipole moment. For a sufficiently fine lattice discretization, this procedure does not result in a significant change in the average magnitude of the random charge distribution. Since the color charges of different nucleons are uncorrelated, the resulting nuclear color charge squared per unit area has a position-dependent magnitude, $\Lambda_s^2(r) = \frac{2}{l} \Lambda_n^2 \sqrt{R^2 - r^2}$, where r is the transverse radial coordinate relative to the beam axis through the center of the nucleus and l is the nucleon diameter. We can adjust Λ_n to ensure the central nuclear color charge squared per unit area $\Lambda_{s0}^2 \equiv \Lambda_s^2(0)$ has a desired value.

Once the color charge distributions of the incoming nuclei are determined, the corresponding classical gauge fields can be computed. The initial conditions for the gauge fields in the overlap region between the nuclei are obtained as discussed previously [20]. For each configuration of color charges sampled, Hamilton's equations are solved on the lattice for the gauge fields and their canonical momenta as a function of the proper time τ .

We first compute the momentum anisotropy parameter α (defined in Fig. 1) as a function of the proper time τ [25]. The results for values of the external parameter $\Lambda_{s0}R = 18.5$ and $\Lambda_{s0}R = 74$ (spanning the RHIC-LHC range of energies) are shown in Fig. 1. We observe that α rises gradually saturating at $\alpha \sim 1\%$ at a proper time on the order of the size of the system. The time required to develop an anisotropy is clearly much larger than the characteristic time $\sim 1/\Lambda_{s0}$ associated with nonlinearities in the system.

The calculation of elliptic flow, defined by Eq. (1), involves determining the gluon number, a quantity whose meaning is ambiguous outside a free theory. Closely following our earlier work [21, 22], we resolve this ambiguity by computing the number in two different ways; directly in Coulomb Gauge (CG) and by solving a system of relaxation (cooling) equations for the fields. Both definitions give the usual particle number in the case of a free theory. We expect the two to be in good agreement for a weakly coupled theory. Wherever the two disagree strongly, we should not trust either.

It is easy to show that $v_2 N$, N being the total gluon number, can be reconstructed from the cooling time history of $T_{xx} - T_{yy}$, just as N can be reconstructed from that of the energy functional [21]:

$$v_2 N = \sqrt{\frac{2}{\pi}} \int_0^\infty \frac{dt}{\sqrt{t}} (T^{xx}(t) - T^{yy}(t)). \quad (2)$$

This expression for $v_2 N$ is manifestly gauge invariant.

In contradistinction to the gluon number, an estimate of v_2 involves both the fields and their conjugate momenta. Indeed, consider the expression for $T_{xx} - T_{yy}$ in our system:

$$T_{xx} - T_{yy} = \int d^2x_\perp [E_y^2 - E_x^2 + (D_x \Phi)^2 - (D_y \Phi)^2],$$

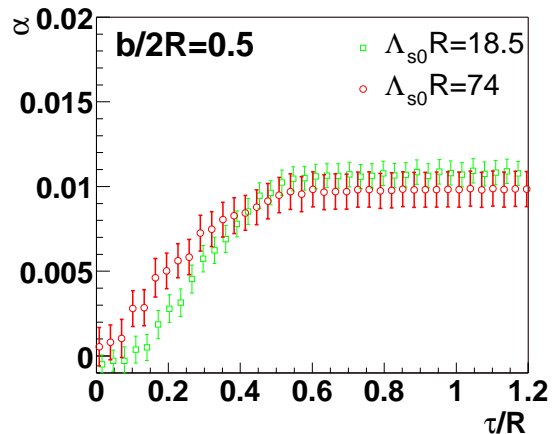


FIG. 1: The momentum anisotropy parameter $\alpha = \langle T^{xx} - T^{yy} \rangle / \langle T^{xx} + T^{yy} \rangle$ for a peripheral nuclear collision corresponding to impact parameter $b/2R = 0.5$ is plotted versus the proper time τ in units of the nuclear radius R for two different values of $\Lambda_{s0}R$.

where \mathbf{E} is the chromo-electric field, Φ the adjoint scalar field, and D_i the covariant derivative, In the weak-coupling limit D_i reduces to ∂_i , the usual derivative. In that limit, the first two terms in $T_{xx} - T_{yy}$ only involve the conjugate momenta of gluons polarized in the transverse plane, while the last two terms only depend on the fields of gluons whose polarization is perpendicular to that plane. Since it is not a priori obvious that the two polarizations contribute equally to v_2 , both the fields and the conjugate momenta should be computed. For the cooling method, relaxation equations for conjugate momenta require that the usual relation between the momenta and *proper* time derivatives of the fields hold at all *cooling* times [26].

In Figure 2, we compare, for a fixed impact parameter ($b/2R = 0.5$), the values of v_2 obtained by the different methods. In the cooling approach, v_2 can be computed first by considering only the potential part of $T_{xx} - T_{yy}$ in Eq. 2 and then assuming an equal contribution from the kinetic part. As seen in Figure 2, such an equality does not hold until very late times. There is a significant difference at early times between the CG and cooling estimates of v_2 .

At asymptotically large cooling times we expect N and $v_2 N$ of the cooled configuration to vanish. If the CG values of these do not vanish, then they are artifacts of the CG. We subtract the residual values from the corresponding values before cooling. The result is referred to as the corrected CG values. The cooling and the CG computations are expected to agree at late times, as the system becomes increasingly weakly coupled. The two methods agree for N at fairly early times. For v_2 , this convergence occurs at much later times, since, as we shall see in the following, v_2 is dominated by very soft modes with

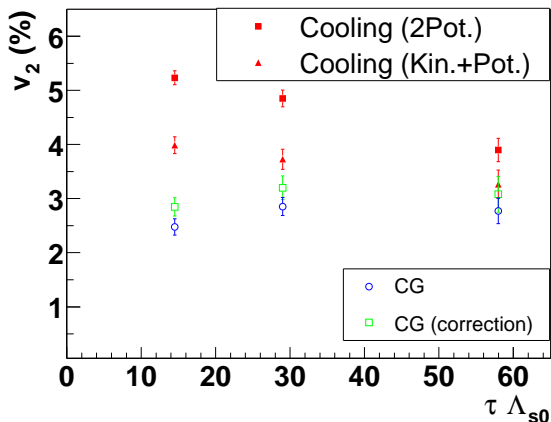


FIG. 2: v_2 is plotted (for impact parameter $b/2R = 0.5$) versus $\Lambda_s \tau$. Solid squares are cooling results using only the potential contribution. Solid diamonds include the contribution of both potential and kinetic terms. The Coulomb gauge result, including both the potential and the kinetic contributions, is shown in open circles. Open squares are corrected CG results-see text for an explanation.

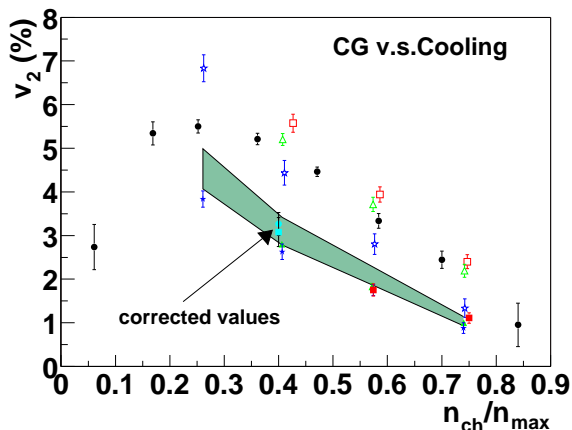


FIG. 3: The centrality dependence of v_2 at the earliest times in Fig. 2 is computed using cooling (open symbols) and CG (filled symbols). Results are for $\Lambda_{s0}R$ spanning the RHIC-LHC range, specifically, $\Lambda_{s0}R = 18.5$ (squares), 37 (triangles), and 74 (stars). Full circles denote *preliminary* STAR data [7]. The band denotes the estimated value of v_2 when extrapolated to very late times. “Corrected values” denotes the late time cooling and CG result for $\Lambda_{s0}R = 18.5$ at one centrality value.

momenta $p_T < \Lambda_{s0}$.

In Figure 3 we plot v_2 reconstructed from the cooling time history of only the potential terms in $T_{xx} - T_{yy}$, along with the CG values (also including potential terms only) as a function of n_{ch}/n_{tot} for different values of $\Lambda_{s0}R$ as discussed in the figure. The systematic errors represented by the band (for $\Lambda_{s0} = 18.5$ [27]) are primarily due to limited resources available to study the slow convergence of the cooling and CG computations. We

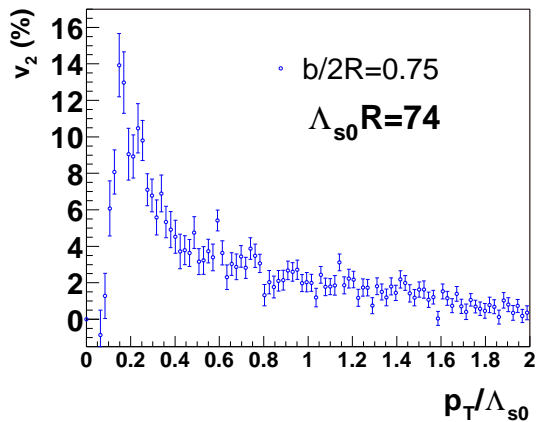


FIG. 4: $v_2(p_T)$ as a function of transverse momentum in dimensionless units for $\Lambda_{s0}R = 74$.

have studied the late time behavior of v_2 for one impact parameter-the results are shown in the figure.

The asymptotic values of v_2 , as predicted by the model, undershoot the data. This disagreement notwithstanding, our results show that a significant v_2 can be generated by the classical fields in the pre-equilibrium stage of a collision. For very peripheral collisions, where the gluon density may be too low to justify the classical approximation, the predictions of the model are not reliable. Interestingly, the dependence of v_2 on $\Lambda_{s0}R$ is rather weak. For a fixed impact parameter, the model predicts that, as $\Lambda_{s0}R \rightarrow \infty$, the classical contribution to the elliptic flow goes to zero. This is because increasing $\Lambda_{s0}R$ is equivalent to increasing R for fixed Λ_{s0} and therefore reducing the initial anisotropy.

In Fig 4, $v_2(p_T)$ is plotted for $b/2R = 0.75$ for $\Lambda_{s0}R = 74$. Our calculations show that the elliptic flow rises rapidly and is peaked for $p_T \sim \Lambda_{s0}/4$ before falling rapidly. The theoretical prediction [28] is that for $p_T \gg \Lambda_{s0}$, $v_2(p_T) \sim \Lambda_{s0}^2/p_T^2$. The numerical data appear to confirm this result-better statistics are required to determine the large momentum behavior accurately. Our p_T distributions clearly disagree with experiment [6, 29]. A couple of comments about our result are in order. Firstly, even though Λ_{s0}^2 is large, it may differ considerably from the color charge squared in the region where the nuclei overlap. This may explain in part why the momenta are peaked at smaller values of p_T . Secondly, the dominant contribution of very soft modes to v_2 helps explain why the cooling and CG computations differ until very late times. The soft gluon modes have large magnitudes and therefore continue to interact strongly until very late proper times. Concomitantly, the occupation number of these modes is not small and the classical approach may be adequate to describe these modes even at the late times considered.

It has been argued by several authors that hydro-

dynamic flow provides a significant contribution to the anisotropy [8]. It is important to emphasize that there may exist a considerable window in time between where the classical approach breaks down and where the system may be considered thermal [30]. A quantitative study of the anisotropy generated in this intermediate regime would therefore be very useful.

Finally, we note that v_2 is extracted only indirectly from a variety of techniques-in particular, two and four particle cumulant analyses [31]. Recently, it has been proposed that non-flow two particle correlations explain the v_2 data [32]. It is unclear whether this model can explain other features of the measured azimuthal anisotropy. In our approach, a procedure very similar to the experimental approach can be followed and two and four particle correlations can be determined. This work will be reported in the near future.

We thank K. Filiminov, U. Heinz, D. Kharzeev, R. Lacey, Z. Lin, L. McLerran, A. Mueller, J.-Y. Ollitrault, K. Rajagopal, J. Rak, S. Voloshin, Nu Xu, E. Shuryak and D. Teaney for useful comments. We also thank Sourendu Gupta for contributing to the early stages of this work. R. V.'s research is supported by DOE Contract No. DE-AC02-98CH10886. A.K. and R.V. acknowledge support from the Portuguese FCT, under grants CERN/P/FIS/40108/2000 and CERN/FIS/43717/2001. R.V. and Y.N. acknowledge RIKEN-BNL for support. A.K. thanks the BNL NTG for hospitality. We also acknowledge support in part of NSF Grant No. PHY99-07949.

-
- [1] G. F. Bertsch and S. Das Gupta, Phys. Rep. **150**, 189 (1988).
- [2] For reviews and recent developments, see *Quark Matter '99* [Nucl. Phys. **A661** (1999)]; *Quark Matter 2001*, [Nucl. Phys. **A698**, (2002)].
- [3] J.-Y. Ollitrault, Phys. Rev. **D46**, 229 (1992).
- [4] S. Voloshin and Y. Zhang, Z. Phys. **C70**, 665 (1996); A.M. Poskanzer and S. Voloshin, Phys. Rev. **C58**, 1671 (1998).
- [5] H. Sorge, Phys. Rev. Lett. **78**, 2309 (1997); Phys. Rev. Lett. **82**, 2048 (1999).
- [6] STAR Collaboration, K.H. Ackermann *et al.*, Phys. Rev. Lett. **86**, 402, (2001).
- [7] We thank R. J. Snellings for providing us with the *preliminary* STAR data on centrality dependence of v_2 .
- [8] P.F.Kolb, P. Huovinen, U. Heinz, and H. Heiselberg, Phys. Lett. **B500**, 232 (2001); D. Teaney, J. Lauret and E. V. Shuryak, Phys. Rev. Lett. **86**, 4783 (2001); arXiv:nucl-th/01110037; *ibid.*, Nucl. Phys. A **698**, 479 (2002); P. F. Kolb, J. Sollfrank, and U. Heinz, Phys. Rev. **C62**, 054909 (2000).
- [9] T. Hirano, Phys. Rev. C **65**, 011901 (2002).
- [10] M. Gyulassy, I. Vitev, X.-N. Wang, Phys. Rev. Lett. **86**, 2537 (2001); X.-N. Wang, Phys. Rev. **C63**, 054902 (2001).
- [11] D. Molnar and M. Gyulassy, Nucl. Phys. A **697**, 495 (2002).
- [12] L.V. Gribov, E. M. Levin and M. G. Ryskin, Phys. Repts. **100** (1983) 1; A. H. Mueller and J.-W. Qiu, Nucl. Phys. **B268**(1986) 427; J. P. Blaizot and A. H. Mueller, Nucl. Phys. **B289** (1987) 847.
- [13] L. McLerran and R. Venugopalan, Phys. Rev. **D49** 2233 (1994); **D49** 3352 (1994); **D50** 2225 (1994); **D59** 094002 (1999); J. Jalilian-Marian, A. Kovner, L. McLerran and H. Weigert, Phys. Rev. **D55** 5414 (1997); Y. V. Kovchegov, Phys. Rev. D **54**, 5463 (1996). J. Jalilian-Marian, A. Kovner, and H. Weigert, Phys. Rev. **D59** 014015 (1999); E. Iancu and L. D. McLerran, Phys. Lett. B **510**, 133 (2001).
- [14] E. Iancu, A. Leonidov and L. McLerran, arXiv:hep-ph/0202270.
- [15] The correct leading logarithmic relation between Λ_s and the gluon saturation scale Q_s is $Q_s^2 = \Lambda_s^2 N_c \ln(\Lambda_s^2/\Lambda_{QCD}^2)/4\pi$. Assuming (for cylindrical nuclei!) that Λ_s has the same x and atomic number dependence as Q_s , the Golec-Biernat-Wusthoff parametrization of HERA data [16] gives $\Lambda_s \sim 1.4$ GeV. Other estimates give $\Lambda_s \sim 2$ GeV [17].
- [16] K. Golec-Biernat and M. Wusthoff, Phys. Rev. D **59** (1999) 014017; A. Stasto, K. Golec-Biernat and J. Kwiecinski, Phys. Rev. Lett. **86** (2001) 596.
- [17] R. Venugopalan, Acta Phys. Polon. B **30**, 3731 (1999).
- [18] A. Kovner, L. McLerran and H. Weigert, Phys. Rev **D52** 3809 (1995); **D52** 6231 (1995). Y. V. Kovchegov and D. H. Rischke, Phys. Rev. **C56** (1997) 1084; M. Gyulassy and L. McLerran, Phys. Rev. **C56** (1997) 2219.
- [19] D. Kharzeev and M. Nardi, Phys. Lett. **B507** (2001), 121; D. Kharzeev and E. Levin, nucl-th/0108006; J. Schaffner-Bielich, D. Kharzeev, L. McLerran, and R. Venugopalan, nucl-th/0108048.
- [20] A. Krasnitz and R. Venugopalan, hep-ph/9706329, hep-ph/9808332; Nucl. Phys. **B557** 237 (1999); Phys. Rev. Lett. **84** (2000) 4309.
- [21] A. Krasnitz and R. Venugopalan, Phys. Rev. Lett. **86** (2001) 1717.
- [22] A. Krasnitz, Y. Nara and R. Venugopalan, Phys. Rev. Lett. **87**, 192302 (2001).
- [23] Our computations are performed for an SU(2) gauge theory. We expect that v_2 , since it is a ratio of components of the stress- energy tensor, will likely be independent of the number of colors.
- [24] C. S. Lam and G. Mahlon, Phys. Rev. D **61**, 014005 (2000); *ibid.*, Phys. Rev. D **62**, 114023 (2000).
- [25] For the case of classical fields, α provides a lower bound on v_2 .
- [26] J. Ambjorn and A. Krasnitz, Nucl. Phys. B **506**, 387 (1997).
- [27] The band will likely be lower for larger values of $\Lambda_s R$.
- [28] D. Teaney and R. Venugopalan, arXiv:hep-ph/0203208.
- [29] S. A. Voloshin, arXiv:nucl-th/0202072.
- [30] R. Baier, A. H. Mueller, D. Schiff and D. T. Son, Phys. Lett. **B502** 51 (2001); *ibid.*, arXiv:hep-ph/0204211.
- [31] N. Borghini, P. M. Dinh and J. Y. Ollitrault, Phys. Rev. C **64**, 054901 (2001); Phys. Rev. C **63**, 054906 (2001).
- [32] Y. V. Kovchegov and K. L. Tuchin, arXiv:hep-ph/0203213.